Photoionization of *N*-alkylphenothiazines in Mesoporous Me-AlMCM-41 Containing Transition Metal Ions Me = Ni(II), Fe(III), and Cu(II)

Sunsanee Sinlapadech, R. M. Krishna, Zhaohua Luan, and Larry Kevan*

Department of Chemistry, University of Houston, Houston, Texas 77204-5641

Received: December 13, 2000; In Final Form: March 9, 2001

Photoionization of *N*-alkylphenothiazines in mesoporous Me-AlMCM-41 containing ion-exchanged transition metal ions Me = Ni(II), Fe(III), and Cu(II) was investigated. *N*-alkylphenothiazine cation radicals ($PC_n^{+\cdot}$) are produced by 320 nm light at room temperature and characterized by electron spin resonance and ultraviolet−visible diffuse reflectance spectroscopy. Me-AlMCM-41 materials are shown to be efficient heterogeneous hosts for the photoinduced formation of long-lived $PC_n^{+\cdot}$ cation radicals, indicating efficient photoinduced charge separation. Ni−AlMCM-41 shows the highest photoionization efficiency compared to Fe−AlMCM-41 and Cu−AlMCM-41. The photoionization efficiency depends on the metal ion type and concentration ion-exchanged into mesoporous Me-AlMCM-41 molecular sieves. Also, as the alkylphenothiazine alkyl chain length increases from methyl to hexadecyl, the photoionization yield decreases.

Introduction

Photoionization with net electron transfer has been a subject of much research. One interesting application involves light energy storage and conversion.[1,2] In a photoredox system, the stored chemical energy of photoproducts serves as an energy source to drive chemical reactions. Back electron transfer must be minimized to achieve a net production of photoproducts. Several photoredox systems have been designed to improve the net energy conversion efficiency.[3−6]

Generally, a photoredox system consists of a photosensitive electron donor and an electron acceptor to generate a pair of radical ions.[7,8] It is desirable to extend the lifetime of the photoinduced radical ions to be able to utilize the stored energy before back electron transfer occurs. Net photoionization efficiency is enhanced in porous materials such as silica gels[9] and zeolites[10] by trapping the electron inside the porous materials.

MCM-41 mesoporous silica molecular sieves were first synthesized by Mobil scientists.[11] MCM-41 materials have uniform pore sizes from 15 to 100 Å, which can be controlled during synthesis.[12,13] Aluminum can substitute for some silicon in MCM-41 to form AlMCM-41, which has a negatively charged framework and net ion-exchange capacity.[14−16] The structures of MCM-41 and AlMCM-41 are hexagonal, as characterized by X-ray powder diffraction (XRD) and nitrogen adsorption techniques.[17−19] One advantage of AlMCM-41 materials over siliceous MCM-41 is that they exhibit greater ion-exchange capacity and acidity.[15,20−23]

MCM-41 and AlMCM-41 are effective catalysts for oxidation reactions[24−27] and are promising host systems for photoredox reactions.[7,28−30] Previous studies showed that MCM-41 and AlMCM-41 can achieve long-lived photoproduced charge separation.[7,30] Incorporation of reducible transition metal ions into silica and aluminosilica porous materials further impedes back electron transfer by acting as a more stable electron acceptor.[7,30,37,38]

Transition metals such as titanium,[7,30] manganese,[31] copper,[32] or vanadium[33] have been incorporated into either framework or extraframework (ion-exchange) sites of MCM-41. Titanium ion [Ti(IV)] has been successfully incorporated into framework sites of MCM-41 and shows high photoionization efficiency for incorporated photoionizable molecules.[7,30] However, photoionization of photoionizable molecules in AlMCM-41 ion-exchanged with different transition metal ions has not yet been studied.

In this work, AlMCM-41 with transition metal ions incorporated by ion-exchange were prepared and denoted as Me-AlMCM-41 [Me = Ni(II), Fe(III) or Cu(II)]. They are used as heterogeneous hosts for photoinduced electron transfer from N-alkylphenothiazines (PC_n, n=1, 6, 10 or 16 where n is the number of carbon atoms in the alkyl chain). The structures, pore sizes, and surface areas of AlMCM-41 with different amounts of Al were characterized by powder X-ray diffraction and N_2 adsorption before ion-exchanging with transition metal ions. The efficiency of photoionization of *N*-alkylphenothiazines incorporated into Me-AlMCM-41 was monitored by electron spin resonance (ESR) and ultraviolet−visible diffuse reflectance spectroscopy. The experimental results show that the photoyields depend on the nature and the amount of metal ions in Me-AlMCM-41 materials. The photoionization of *N*-alkylphenothiazines with different alkyl chain lengths was also compared.

Experimental Section

Synthesis of AlMCM-41. Commercial trimethylammonium hydroxide (Aldrich), sodium silicate solution (27 wt % SiO_2; Aldrich), cetyltrimethylammonium bromide (Aldrich), fumed silica (Aldrich), and aluminum sulfate (Fluka) were used as received for AlMCM-41 synthesis. AlMCM-41 materials with different Al contents (Si/Al = 15, 30, and 60) were prepared hydrothermally using cetyltrimethylammonium bromide as the organic template following an earlier procedure.[15]

In brief, 10 g of trimethylammonium hydroxide was mixed with 2.95 g of sodium silicate solution and 10 g of distilled water. Cetyltrimethylammonium bromide (4.3 g) was dissolved in 43 g distilled water and slowly added to the mixture. To this mixture, fumed silica was added and stirred for 1 h. Aluminum

10.1021/jp0044882 CCC: $20.00
Published on Web 04/19/2001

sulfate (0.12, 0.25 or 0.51 g) was dissolved in 15 g water and added to the mixture. The pH of the mixture was adjusted to 11.5 using 2 M H_2SO_4. All these samples were autoclaved in Teflon bottles for 2 days near 100 °C. After crystallization, the solid product was filtered at room temperature. The solid product was washed with distilled water and dehydrated in an oven at 85 °C in air for about 5 h. The solid powder was calcined at 550 °C for 12 h to remove water and organic templates.

Characterization. Powder X-ray diffraction (XRD) patterns of AlMCM-41 were obtained with a Philips PW 1840 diffractometer using Cu Ka radiation of wavelength 1.541 Å over the range $1.5° < 2\theta < 15°$. Structure type, crystallinity, and phase purity of AlMCM-41 with different Al contents were confirmed by XRD and the Al content was measured by electron microprobe analysis on a JXA-8600 spectrometer.

Nitrogen adsorption isotherms were measured at 77 K using a Micromeritics Gemini 2375 analyzer. The volume of adsorbed N_2 was normalized to standard pressure and temperature. Prior to the experiments, samples were dehydrated at 250 °C for 1 h. The specific area, A_{BET}, was determined from the linear part of the BET equation. The Barrett−Joyner−Halenda (BJH) method[34,35] was used to determine the cumulative pore surface area (A_{BJH}), pore volume (V_{BJH}) and pore sizes (D_{BJH}) of AlMCM-41 samples. A_{BJH} and V_{BJH} were obtained from the pore size distribution curves, whereas D_{BJH} was calculated from 4 V_{BJH}/A_{BJH}.

The ESR spectra were recorded at room temperature at X-band frequency using a Bruker ESP 300 spectrometer with 100 kHz field modulation and microwave power low enough to avoid saturation and distortion of the spectrum. The photoproduced $PC_n^{+\cdot}$ (n=1, 6, 10 or 16) radical yields were determined by double integration of the ESR spectra using the ESP 300 software. Diffuse reflectance ultraviolet−visible spectra were recorded before and after different times of 320 nm photoirradiation at room temperature using a Perkin-Elmer model 330 spectrophotometer with an integrating sphere accessory. Thermogravimetric analysis (TGA) of the samples were performed using a TGA 2050 analyzer from TA Instruments.

Ion-Exchange of AlMCM-41. $Cu(NO_3)_2$ (Fisher-Scientific), $Ni(NO_3)_2$ (Acros) and $Fe(NO_3)_3$ (Fisher-Scientific) were used as received for ion-exchange. To study the effect of transition metal ions on the photoyield, 0.5 M of metal ion solutions of $Cu(NO_3)_2$, $Ni(NO_3)_2$, and $Fe(NO_3)_3$ were liquid-state ion-exchanged with calcined AlMCM-41 (Si/Al = 30). The mixtures were stirred near 90 °C for 1 h according to procedures described.[32] To explore whether the photoyield depends on the amount of the transition metal ion contained in Me-AlMCM−41, different ratios of AlMCM-41 (Si/Al = 15, 30, and 60) were liquid-state ion-exchanged with 0.5 M $Ni(NO_3)_2$. The nickel ion contents in Ni−AlMCM-41 were determined by electron microprobe analysis using a JEOL JXA-8600 spectrometer.

Photoionization Samples. Methylphenothiazine was used as received from Aldrich. Hexylphenothiazine (PC_6), decylphenothiazine (PC_{10}), and hexadecylphenothiazine (PC_{16}) were synthesized following a reported procedure.[8] The ion-exchanged solids Me-AlMCM-41 were heated at 550 °C for 1 h to remove water and organic templates. They were then transferred to a glovebox under N_2 flow. The ion-exchanged solids (Me-AlMCM-41) were impregnated with *N*-alkylphenothiazines in a glovebox at room temperature by mixing Me-AlMCM-41 (0.1 g) with 1 mL of 0.01 M *N*-alkylphenothiazines in benzene for 30 min in the dark. The benzene was evaporated by flowing dry nitrogen gas over the samples in a glovebox for 2 h. For electron spin resonance measurements, the solid powders were introduced into 2 mm i.d. x 3 mm o.d. Suprasil quartz tubes and sealed with Parafilm.

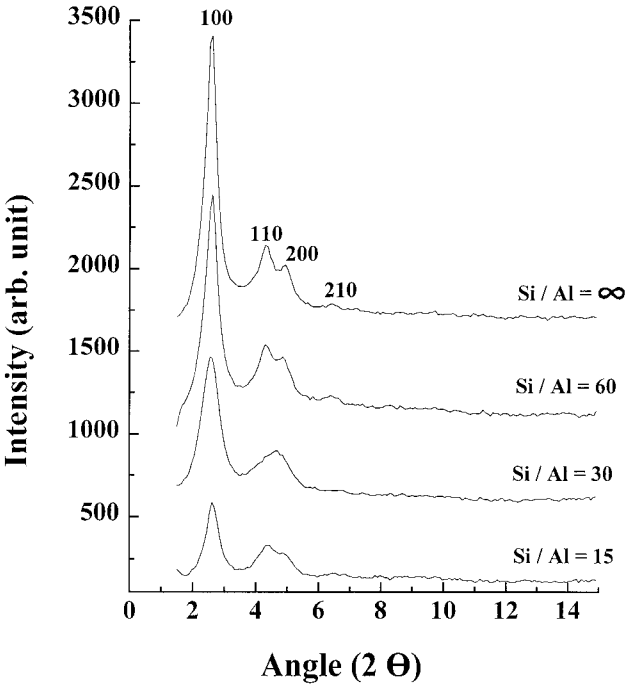

Figure 1. XRD patterns of calcined MCM-41 and AlMCM-41.

For diffuse reflectance measurements, the samples were filled into a cylindrical quartz sample cell (20 mm diameter by 1 mm path length) which was evacuated to below 1 Torr and sealed with Parafilm. All samples were handled in the dark to minimize exposure to light.

Photoionization Procedures. Each powder was photoirradiated at room temperature with a Cermax 150 W xenon lamp (ILC-LX150 F). The light was passed through a 10 cm water filter and a Corning glass filter 7−51 with 90% transparency at 240 and 400 nm and a maximum at 320 nm. The samples were rotated during photoirridiation for uniform exposure to the light. ESR was used to detect the photoproduced *N*-alkylphenothiazine cation radicals. The cation radical yields ($PC_n^{+\cdot}$, where n = 1, 6, 10 or 16) produced from the reaction were determined by ESR and diffuse reflectance ultraviolet−visible spectroscopy.

Results

The XRD patterns of calcined AlMCM-41 with different Si/Al ratios and siliceous MCM-41 are consistent with previous reports[11,12,15] as shown in Figure 1. No impurity phase was detected. The reflections at 100, 110, 200, and 210 indicate a hexagonal structure for the AlMCM-41 materials. The XRD peaks of AlMCM-41 materials become broader and less resolved as the Al loading increases. Table 1 shows the BET surface areas, BJH surface areas, volume absorbed (V_{BJH}) and pore sizes of AlMCM-41 with different Al contents. The increase of Al content in AlMCM-41 results in a decrease of the A_{BET} and A_{BJH} surface areas. However, the pore sizes (D_{BJH}) for different Si/Al ratios in AlMCM-41 are similar (27−29 Å) except for the highest Al content which shows a larger pore size (38 Å). It is not expected that the metal ion-exchanged into AlMCM-41 affects the pore size or structure.

Methylphenothiazine and its derivatives are important molecules due to their antioxidant and electron donor properties. The diameters of PC_1, PC_6, PC_{10}, and PC_{16} molecules are about 6.5, 10.5, 14.5, and 20 Å, respectively.[30] This means that the

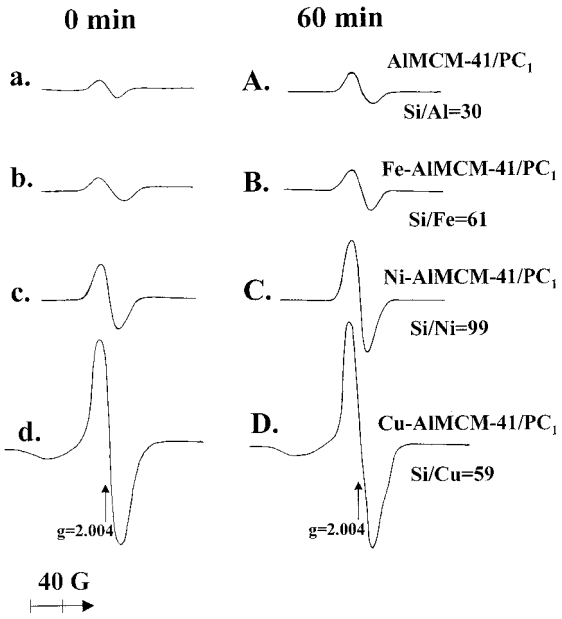

Figure 2. ESR spectra of $PC_1^{+\cdot}$ in Me-AlMCM-41/PC_1 [Me = Cu(II), Fe(III), or Ni(II)] at 0 and 60 min irradiation time with 320 nm light at room temperature.

TABLE 1: Pore Structure Parameters of AlMCM-41 Calculated from the Desorption Branch of Nitrogen Adsorption Isotherms

materials	A_{BET} (m^2g^{-1})	A_{BJH} (m^2g^{-1})	D_{BJH} (Å)	V_{BJH} (cm^3g^{-1})
AlMCM-41 (Si/Al = 15)	701	851	38	0.7
AlMCM-41 (Si/Al = 30)	930	1079	29	0.8
AlMCM-41 (Si/Al = 60)	978	1095	29	0.8
AlMCM-41 (Si/Al = ∞)	1264	1193	27	0.9

cage openings of AlMCM-41 seem big enough to be occupied by *N*-alkylphenothiazines (PC_n where n=1, 6, 10, or 16). But thermogravimetric analysis results (see below) indicate that this is not completely true for all these alkyl chain lengths. Incorporation of methylphenothiazine (PC_1) into Me-AlMCM-41 [Me = Ni(II), Fe(III), or Cu()] produces a background ESR signal of methylphenothiazine cation radicals ($PC_1^{+\cdot}$) as shown in Figure 2. The samples are light pink before irradiation (Fig 2a−d) and turn dark pink after irradiation (Fig 2A−D). The pink color is characteristic of $PC_1^{+\cdot}$ cation radicals.[8,9] The unresolved signal with a *g* value of 2.004 is assigned to $PC_1^{+\cdot}$ following previous literature.[8,9] From Figure 3, it is evident that the ESR signal intensities of the $PC_1^{+\cdot}$ radical ions dramatically increase during the first 10 min and reach a plateau in about 60 min by 320 nm photoirradiation. Cu−AlMCM-41 produces the highest dark reaction compared to Ni−AlMCM-41 and Fe−AlMCM-41. The highest net photoyield is obtained for Ni−AlMCM-41 followed by Fe−AlMCM-41, Cu−AlMCM-41 and AlMCM-41. The photoyields of Me-AlMCM-41 decrease during the first 3 h and then remain relatively stable for several days.

The diffuse reflectance ultraviolet spectra of AlMCM-41 (Si/Al = 15) with impregnated PC_1 is shown in Figure 4. The pink color characteristic of $PC_1^{+\cdot}$ cation radicals [8,9] is also observed before irradiation and shows absorption in the visible (515 nm). This also supports the fact that some PC_1 is ionized to $PC_1^{+\cdot}$ during sample preparation. From Figure 4, the photoyield rapidly increases during the first 10 min irradiation by 320 nm light at room temperature. For AlMCM-41 with impregnated PC_{16} (not

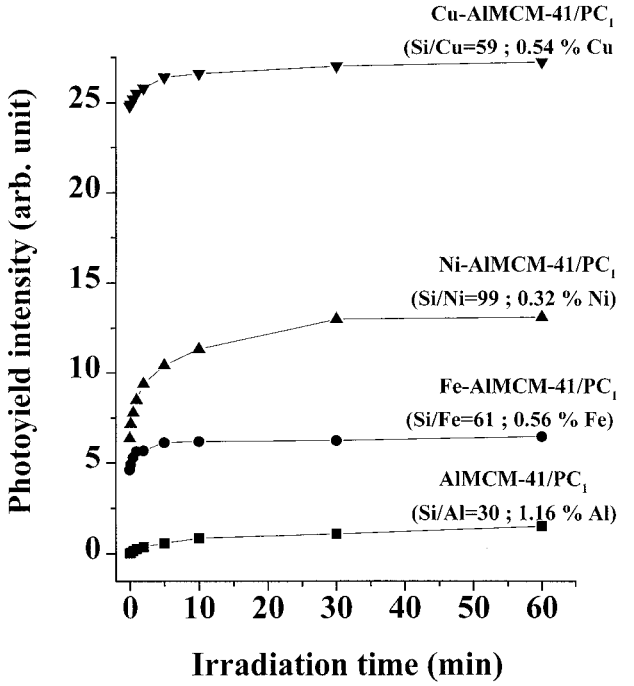

Figure 3. ESR intensity of $PC_1^{+\cdot}$ in Me-AlMCM-41/PC_1 [Me = Cu(II), Fe(III), or Ni(II)] versus 320 nm irradiation time at room temperature.

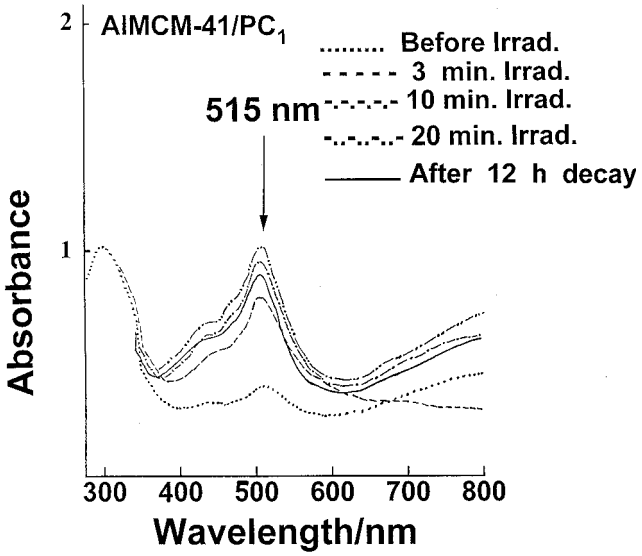

Figure 4. Diffuse reflectance ultraviolet spectra of AlMCM-41/PC_1 at room temperature before irradiation, and after 320 nm light irradiation for 3, 10, and 20 min and after subsequent decay for 12 h.

shown), a weak absorption at 515 nm is observed prior to irradiation. The $PC_{16}^{+\cdot}$ intensity in AlMCM-41/PC_{16} slowly increases as the irradiation time increases. For Ni−AlMCM-41 (Si/Ni = 64), a weak absorption peak was also observed at 515 nm before photoirradiation. The peak intensity significantly increases after 3 min irradiation and then gradually increases until 20 min irradiation as shown by Figure 5. This confirms that PC_1 is photoionized to $PC_1^{+\cdot}$ radical ions by 320 nm light. As compared to AlMCM-41 impregnated with PC_1, the net photoyield of Ni−AlMCM-41 is about 1.5 times larger than that of AlMCM-41 after 20 min. irradiation time at room temperature.

Figure 6 shows the photoyield of $PC_1^{+\cdot}$ in Ni−AlMCM-41/PC_1 with different Ni(II) concentrations and different irradiation times. The highest Ni(II) content yields the highest dark reaction

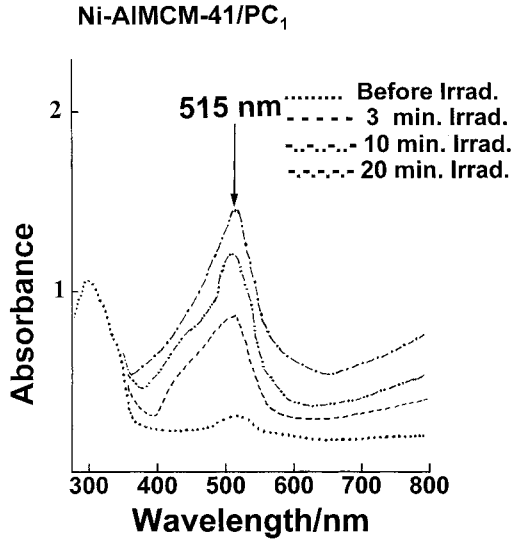

Figure 5. Diffuse reflectance ultraviolet spectra of Ni−AlMCM-41/PC_1 at room temperature before irradiation and after 3, 10, and 20 min irradiation with 320 nm light at room temperature.

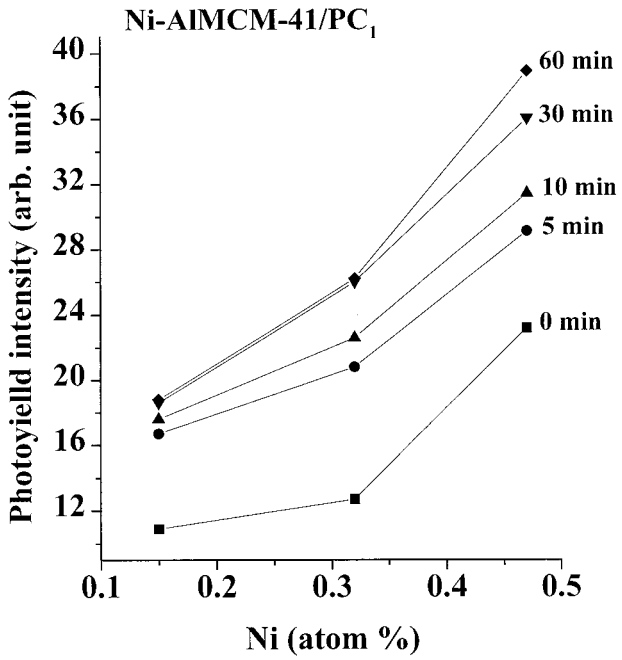

Figure 6. Dependence of ESR intensity of $PC_1^{+\cdot}$ in Ni−AlMCM-41/PC_1 with different Ni(II) concentrations versus 320 nm irradiation time at room temperature.

prior to irradiation. The photoyield intensity of $PC_1^{+\cdot}$ increases with increasing irradiation time. Moreover, it is also dependent on the Ni(II) concentration in Ni−AlMCM-41. At low Ni content (0.15% Ni), the photoyield seems rather constant after 5 min photoirradiation at room temperature. For higher Ni contents, the photoyields still increase after 5 min and reach a plateau after about 30 min photoirradiation. After 60 min irradiation, the photoyields of $PC_1^{+\cdot}$ in Ni−AlMCM-41/PC_1 increase 68% for 0.15% Ni, 106% for 0.32% Ni, and 72% for 0.47% Ni.

ESR signals of *N*-alkylphenothiazine cation radicals ($PC_n^{+\cdot}$; n=1, 6, 10, or 16 where n is the number of carbon atoms in the alkyl chain) in Ni−AlMCM-41 (Si/Ni = 99) are observed. As one can see from the Figure 7, the dark reaction becomes less as the alkyl chain length increases. All samples exhibit a photoyield when irradiated by 320 nm light for 60 min. Figure 7 shows that the ESR intensities of the $PC_n^{+\cdot}$ ions increase as

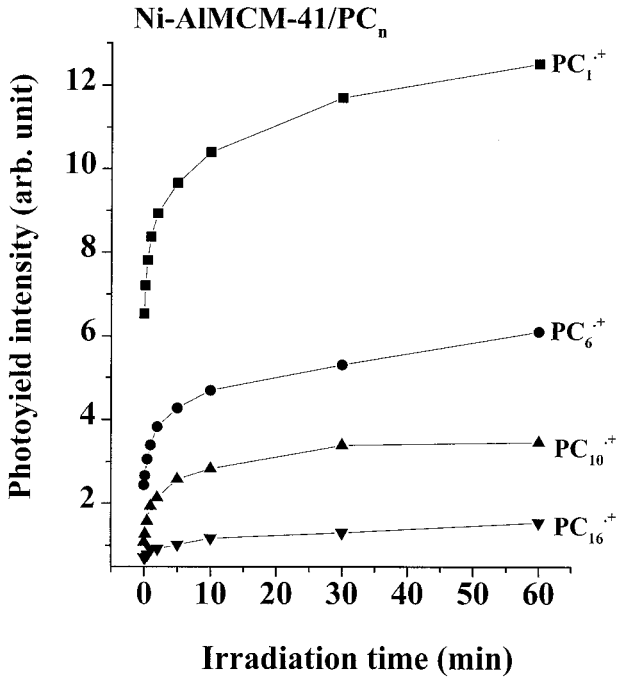

Figure 7. ESR intensity of $PC_n^{+\cdot}$ in Ni−AlMCM-41/PC_n (n = 1, 6, 10, or 16; Si/Ni = 99) versus 320 nm irradiation time at room temperature.

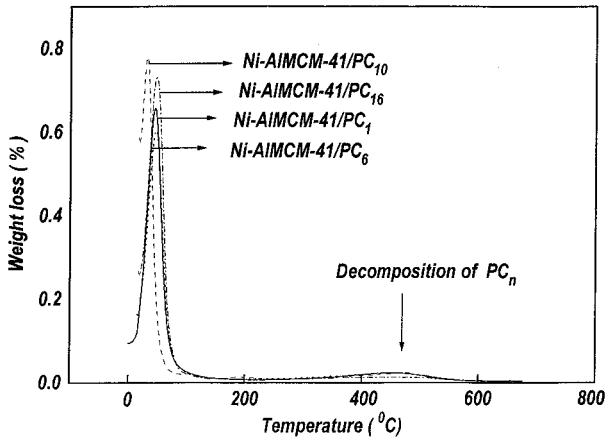

Figure 8. TGA curves in flowing oxygen of Ni−AlMCM-41/PC_n (Si/Ni = 99) materials.

the 320 nm irradiation time increases until they reach a plateau after about 1 h. These photoyields are stable at room temperature for several days.

Thermogravimetric Analysis (TGA). The TGA curves for Ni−AlMCM-41 (Si/Ni = 99) with different alkyl chain lengths of *N*-alkylphenothiazines are shown in Figure 8. All TGA curves show peaks near 50−80 °C that are assigned to weight losses due to water. The TGA curves show an additional broad peak near 475 °C that is assigned to oxidative decomposition of phenothiazine derivatives inside the Ni−AlMCM-41 channels.[36−38] As one can see from Figure 8, oxidative decomposition of PC_1, PC_6, PC_{10}, and PC_{16} is observed near 475 °C although the peak for $PC_{16}^{+\cdot}$ is very small.

Discussion

XRD and N_2 adsorption experiments suggest that the cage sizes of AlMCM-41 are big enough to be occupied by *N*-alkylphenothiazines (PC_n) for n up to 16. This conclusion is modified by the interpretation of the broad TGA peaks near

475 °C (Figure 8), which are assigned to oxidative decomposition of PC_n **inside** Ni−AlMCM-41,[36,37] observed for all *N*-alkylphenothiazines. From these data, we confirm that **most** of the PC_1 and PC_6 penetrate into the Me-AlMCM-41 channels, whereas PC_{10} and PC_{16} only **partly** penetrate into Me-AlMCM-41 channels, with the rest of the PC_{10} and PC_{16} likely being adsorbed on the external surface of Ni−AlMCM-41.

ESR ($g = 2.004$) and diffuse reflectance (515 nm) signals of methylphenothiazine cation radicals are observed before photoirradiation. This implies that there is some electron transfer from PC_n to Me-AlMCM-41 during the sample preparation process,[7,9,30] which is defined as a dark reaction prior to irradiation. The photoyields of $PC_1^{+\cdot}$ in Me-AlMCM-41/PC_1 increase after photoirradiation based on both ESR and diffuse reflectance, indicating that methylphenothiazine (PC_1) is photoionized to methylphenothiazine cation radicals ($PC_1^{+\cdot}$) by 320 nm photoirradiation.

Relative mobilities of the $PC_n^{+\cdot}$ cation radicals can be estimated by the relative resolution of the ESR spectra.[8,9] The observed unresolved ESR signals of $PC_n^{+\cdot}$ cation radicals in Me-AlMCM-41 [Me = Ni(II), Fe(III), and Cu(II)] indiate that the mobility of $PC_n^{+\cdot}$ cation radicals is restricted which is consistent with them being partly located inside the channels of the Me-AlMCM-41 materials.

One can conclude that the transition metal ions act as electron acceptors from the fact that there is more net photoionization from PC_n in the metal-containing Me-AlMCM-41 materials than in AlMCM-41 materials. Figure 3 shows that Me-AlMCM-41/PC_1 gives higher photoyields as compared with AlMCM-41/PC_1. The photoyield of $PC_1^{+\cdot}$ in Ni−AlMCM-41/PC_1 is the largest as compared with Fe−AlMCM-41 and Cu−AlMCM-41. This suggests that Ni(II) is the most efficient electron acceptor among Ni(II), Fe(III), and Cu(II).

The stabilities of $PC_1^{+\cdot}$ in Ni−AlMCM-41, Fe−AlMCM-41, and Cu−AlMCM-41 are comparable. They all show higher stability as compared with AlMCM-41. Overall, incorporation of a metal ion electron acceptor into ion-exchange sites creates a system where light energy can be converted into chemical energy and stored for a period of time. During the photoionization of Me-AlMCM-41 [Me = Ni(II), Fe(III), and Cu(II)], it is suggested that the transition metal ions accept electrons and are reduced to Ni(I), Fe(II), and Cu(I). Thus, one expects to see an ESR signal of paramagnetic Ni(I) after photoionization. Attempts to detect paramagnetic species were not successful apparently because of overlap with the ESR spectra of $PC_n^{+\cdot}$. However, in a similar photoionization system,[39] ESR has directly shown the photoreduction of V(V) to paramagnetic V(IV) indicating that V(V) acts as an electron acceptor.

The photoyield of $PC_1^{+\cdot}$ in Ni−AlMCM-41/PC_1 depends on the Ni(II) content in Ni−AlMCM-41 as shown in Figure 6. The higher the Ni(II) content the more dark reaction occurs. The photoionization efficiency of PC_1 in Ni−AlMCM-41 materials increases with increasing irradiation time. The highest Ni(II) content shows an increased photoyield for a longer irradiation time (~10 min) at room temperature compared to the lowest Ni content (~5 min.). The role of transition meal ions as electron acceptors is evident since there is net photoionization of PC_n in Me-AlMCM-41 in addition to the dark reaction yield at 0 min photoirradiation observed which varies with the amount of the transition metal ion. The result in Figure 6 also shows that the dark reaction, which is highest for the highest Ni loading, limits the photoionization efficiency of Ni−AlMCM-41 because the highest net photoyield is obtained for the 0.32% Ni in Ni−AlMCM-41, which is an intermediate Ni concentration. Overall, the amount of Ni(II) ion-exchanged into extraframework sites of AlMCM-41 should be high enough to accept an electron from PC_n and create charge separation. However, less dark reaction is desirable to obtain higher photoyields.

Longer alkyl chains on PC_n decrease the photoionization efficiency of *N*-alkylphenothiazines. A longer alkyl chain length makes the molecules more bulky and more difficult to penetrate into the Ni−AlMCM-41 channels. This is confirmed by TGA analysis in which broad peaks near 475 °C assigned to $PC_n^{+\cdot}$ radical ions inside the AlMCM-41 channels are weaker with increasing alkyl chain length. With a sufficiently long alkyl chain, it is expected that the rate of diffusion of the PC_n into Me-AlMCM-41 will be reduced and yield less dark reduction. This explains the photoionization results which show decreased photoyield with longer akyl chain length. The photoyield decreases with increasing alkyl chain length may also be partially due to an increase of molecular aggregate generation with alkyl chain length.[36,40] The formation of such aggregates will further lower the rate of diffusion of PC_n into Me-AlMCM-41 and lead to diminished photoyields.

Conclusions

The experimental data clearly reveal that *N*-alkylphenothiazines incorporated into Me-AlMCM-41 [Me = Ni(II), Fe(III), or Cu(II)] can be photoionized and form alkylphenothiazine cation radicals ($PC_n^{+\cdot}$). Electron transfer seems to occur from PC_n inside the Me-AlMCM-41 channels to the incorporated metal ion, according to ESR and diffuse reflectance spectroscopy. Back electron transfer is efficiently retarded in Me-AlMCM-41. Ni(II) is the most efficient electron acceptor among Ni(II), Fe(III), and Cu(II) ion-exchanged into AlMCM-41. The photoyield depends on the nature and amount of the transition metal ion-exchanged into AlMCM-41, and also on the size of the electron donor molecules.

Acknowledgment. This research was support by the Division of Chemical Sciences, Office of Basic Energy Sciences, Office of Energy Research, U.S. Department of Energy, the Texas Advanced Research Program and the Environmental Institute of Houston.

References and Notes

(1) Kavarnos, G. J.; Turro, N. J. *Chem. Rev.* **1986**, *86*, 401.
(2) Connolly, J. S. *Photochemical Conversion and Storage of Solar Energy*; Academic: New York, 1981.
(3) Vermeulen, L. A.; Thompson, M. E. *Nature* **1992**, *358*, 656.
(4) Nakato, T.; Kazuyuki, K.; Koto, C. *Chem. Mater.* **1992**, *4*, 128.
(5) Kang, Y. S.; McManus, H. J. D.; Kevan, L. *J. Phys. Chem.* **1993**, *97*, 2027.
(6) Yonemoto, E. H.; Kim, Y. I.; Schmehl, R. H.; Wallin, J. O.; Shoulders, B. A.; Richadson, B. R.; Haw, J. F.; Mallouk, T. E. *J. Am. Chem. Soc.* **1994**, *116*, 10 557.
(7) Sung-Suh, H. M.; Luan, Z.; Kevan, L. *J. Phys. Chem. B* **1997**, *101*, 10 455.
(8) Krishna, R. M.; Kurshev, V.; Kevan, L. *Phys. Chem. Chem. Phys.* **1999**, *1*, 2833.
(9) Xiang, B.; Kevan, L. *Langmuir* **1994**, *10*, 2688.
(10) Ledney, M.; Dutta, P. K. *J. Am. Chem. Soc.* **1995**, *117*, 7687.
(11) Kresge, C. T.; Leonowicz, W. J.; Roth, W. J.; Vartuti, J. C.; Beck, J. S. *Nature* **1992**, *359*, 710.
(12) Beck, J. S.; Vartuli, J. C.; Roth, W. J.; Leonowicz, M. E.; Kresge, C. T.; Schmitt, K. D.; Chu, C. T.; Olson, D. H.; Sheppard, E. W.; McCulley, S. B.; Higging, J. B.; Schlenker, J. L. *J. Am. Chem. Soc.* **1992**, *114*, 10 834.
(13) Ying, J. Y.; Mehnert, C. P.; Wong, M. S. *Angew. Chem., Int. Ed.* **1999**, *38*, 56.
(14) Boger, T.; Roesky, R.; Gläser, R.; Ernst, S.; Eigenberger, G.; Weitkamp, J. *Microporous Mater.* **1997**, *8*, 79.
(15) Luan, Z.; Cheng, C.-F.; Zhou, W.; Klinowski, J. *J. Phys. Chem.* **1995**, *99*, 1018.

(16) Biz, S.; White, M. G. *J. Phys. Chem. B* **1999**, *103*, 8432.
(17) Anderson, M. T.; Martin, J. E.; Odinek, J. E.; Newcomer, J. G. *Chem. Mater.* **1998**, *10*, 1490.
(18) Franke, O.; Schulz-Ekloff, G.; Rathousky, J.; Starek, J.; Zukal, A. *J. Chem. Soc., Chem. Commun.* **1993**, 724.
(19) Beck, J. S.; Vartuli, J. C.; Kennedy, G. J.; Kresge, C. T.; Roth, W. J.; Schramm, S. E. *Chem. Mater.* **1994**, *6*, 1816.
(20) Reddy, K. R.; Araki, N.; Niwa, M. *Chem. Lett.* **1997**, *7*, 637.
(21) Corma, A.; Fornes, V.; Navarro, M. T.; Perez-Pariente, J. *J. Catal.* **1994**, *148*, 569.
(22) Mokaya, R.; Jones, W.; Luan, Z.; Alba, M. D.; Klinowski, J. *Catal. Lett.* **1996**, *37*, 113.
(23) Mokoya, R.; Jones, W. *Chem. Commun.* **1997**, *22*, 2185.
(24) Climent, M. J.; Corma, A.; Iborra, S.; Miquel, S.; Primo, J.; Rey, F. *J. Catal.* **1999**, *183*, 76.
(25) Kageyama, K.; Ogino, S.; Aida, T.; Tatsumi, T. *Macromolecules* **1998**, *31*, 4069.
(26) Chaudhari, K.; Das, T. K.; Chandwadkar, A. J.; Sivasanker, S. *J. Catal.* **1999**, *1*, 81.
(27) Long, R. Q.; Yang, R. T. *Ind. Eng. Chem. Res.* **1999**, *38*, 873.
(28) Corma, A.; Fornes, V.; Garcia, H.; Miranda, M. A.; Sabater, A. *J. Am. Chem. Soc.* **1994**, *116*, 9767.
(29) Cano, M. L.; Cozens, F. L.; Garcia, H.; Marti, V.; Scaiano, J. C. *J. Phys. Chem.* **1996**, *100*, 18 152.
(30) Krishna, R. M.; Prakash, A. M.; Kevan, L. *J. Phys. Chem. B* **2000**, *104*, 1796.
(31) Xu, J.; Luan, Z.; Wasowicz, T.; Kevan, L. *Microporous Mesoporous Mater.* **1998**, *22*, 179.
(32) Luan, Z.; Xu, J.; Kevan, L. *Nukleonika* **1997**, *42*, 493.
(33) Luan, Z.; Xu, J.; He, H.; Klinowski, J.; Kevan, L. *J. Phys. Chem.* **1996**, *100*, 19 595.
(34) Ravikovitch, P. I.; Wei, D.; Chueh, W. T.; Haller, G. L.; Neimark, A. V. *J. Phys. Chem. B.* **1997**, *101*, 3671.
(35) Barrett, E. P.; Joyner, L. G.; Halenda, P. P. *J. Am. Chem. Soc.* **1951**, *73*, 373.
(36) Krishna, R. M.; Chang, Z.; Choo, H.; Ranjit, K. T.; Kevan, L. *Phys. Chem. Chem. Phys.* **2000**, *2*, 3335.
(37) Kurshev, V.; Prakash, A. M.; Krishna, R. M.; Kevan, L. *Microporous Mesoporous Matls.* **2000**, *34*, 9.
(38) Ranjit, K. T.; Chang, Z.; Krishna, R. M.; Prakash, A. M.; Kevan, L. *J. Phys. Chem. B* **2000**, *104*, 7981.
(39) Chang, Z.; Ranjit, K. T.; Krishna, R. M.; Kevan, L. *J. Phys. Chem. B* **2000**, *104*, 5579.
(40) Cavanaugh, J. *J. Am. Chem. Soc.* **1959**, *81*, 2507.